Journal of Environmental Monitoring

Cite this: *J. Environ. Monit.*, 2011, **13**, 1589

www.rsc.org/jem

PAPER

Fugacity approach to evaluate the sediment–water diffusion of polycyclic aromatic hydrocarbons

De-Gao Wang,*[ab] Mehran Alaee,[b] Jonathan Byer,[cb] Yong-Jun Liu[a] and Chong-Guo Tian[d]

Received 7th December 2010, Accepted 1st April 2011
DOI: 10.1039/c0em00731e

Diffusion is an important process for sediment-water exchange and plays a vital role in controlling water quality. Fugacity fraction (*ff*) was used to estimate the sediment–water diffusion of polycyclic aromatic hydrocarbons (PAHs) between seawater and surficial sediment. A total of 33 surface sediment and sea water samples were collected concurrently from the northeast coastal area in China and 25 PAHs were analyzed including the alkylated and chlorated PAHs. Fugacity fraction was calculated based on the PAH concentrations in water and sediment, octanol–water partition coefficient of PAHs, organic matter content in sediment, and density of sediment. The calculated results showed that *ff* increased with decreasing molecular weight of PAHs. The low molecular weight PAHs (2–3 rings) transferred from sediment to water and the sediment acted as a secondary source to the water. The medium molecular weight PAHs (4–5 rings) were close to the sediment–water equilibrium and the transfer tendency shifted between sediment and water. The high molecular weight PAHs (5–6 rings) transferred from water into sediment and the sediment acted as a sink. Soot carbon and the difference of PAH concentrations between sediment and water were found to be important factors affecting the sediment–water diffusion. This study provided new insight into the process of sediment–water diffusion, which has a great influence on the quality of water, especially in severely-polluted sediment areas.

Introduction

Polycyclic aromatic hydrocarbons (PAHs) containing two or more fused aromatic rings are ubiquitous pollutants with significant public health and environmental concern. Knowledge of the behavior and fate of PAHs is necessary for accurate exposure and risk assessment. PAHs formed during the incomplete combustion of all types of organic matter are emitted as airborne pollutants associated with particles or directly as volatile pollutants from anthropogenic and natural sources. PAHs can enter the aquatic environment through direct input from urban sewage and run-off or indirect atmospheric dry and wet deposition.[1–3] Once introduced into water, PAHs with high octanol–water partition coefficients (K_{OW}) are easily accumulated in sediment due to their hydrophobic characters. Because of the tendency of hydrophobic pollutants sorbed to organic matter and soot carbon, sediments are the ultimate repository for most organic contaminants, which induce the risk to ecosystem in the aquatic environment.[1,4]

Information on direction across the sediment and water interface is frequently important in water quality assessment or prediction.[4] Sediment–water exchange is one of the most important processes determining the environmental fate and direct or indirect human exposure to PAHs. In the aquatic

[a]*Department of Environmental Science and Engineering, Dalian Maritime University, Dalian, P. R. China. E-mail: degaowang@163.com; Fax: +86-411-8472-8489; Tel: +86-411-8472-8489*
[b]*Water Science and Technology Directorate, Science and Technology Branch, Environment Canada, Burlington, Canada*
[c]*Department of Chemistry, Queen's University, Kingston, Canada*
[d]*Yantai Institute of Coastal Zone Research, Chinese Academy of Sciences, Yantai, P. R. China*

Environmental impact

Sediment–water diffusion plays a vital role in controlling the water quality. However, little information on the sediment–water diffusion of polycyclic aromatic hydrocarbons (PAHs) was available in the real environment from lack of a reliable model. A fugacity fraction approach was developed and used to assess the sediment–water diffusion of PAHs between seawater and surficial sediment based on the field experimental data. This newly developed model can be used in the assessment of sediment–water diffusion for not only PAHs but also other persistent organic substances.

environment, PAHs with varied physicochemical properties have different environmental fate. PAHs with three rings or more have low water solubility and low vapor pressure. As molecular weight increases, water solubility decreases and vapor pressure decreases. PAHs with two rings are more soluble in water and more volatile.

In recent years, numerous studies have focused on soil–air and water–air exchange of many typical persistent toxic pollutants such as PAHs, polychlorinated biphenyls (PCBs), polychlorinated dibenzo-*p*-dioxins (PCDDs), and organochlorine pesticides (OCPs).[5–18] However, the sediment–water exchange of PAHs was scarcely reported in these studies. Sediment–water exchange includes two main processes: (a) particle-phase PAH deposition and resuspension, and (b) the diffusion of dissolved PAHs between sediment and the water column.[19,20] Previous studies focused mainly on the particle-phase deposition of PAHs in water.[21,22] Jeremiason *et al.*[21] studied the setting flux of PAHs sorbed to setting particles using a sediment trap in Lake Superior. They found that the flux of PAHs ranged from 130 ng m^{-2} d^{-1} for phenanthrene to 6 ng m^{-2} d^{-1} for indeno(1,2,3-cd) pyrene, indicating net PAH deposition from water to sediment. Palm *et al.*[22] studied bulk atmospheric deposition fluxes, air–water exchange fluxes, particle settling fluxes out of the upper water column, sediment trap fluxes in deep waters, and sediment burial fluxes of PAHs. All of the transport processes in water were considered in their research except for the process of dissolved sediment–water diffusion of PAHs.

The process of sediment–water diffusion can only be considered in a multimedia model.[4,19,23,24] Jurado *et al.*[4] developed a dynamic coupled hydrodynamic-contaminant model and applied to a Mediterranean continental shelf environment. They found the sediment–water diffusion play a more important role than sink in controlling the concentration of PCB 28 in bottom seawater.[4] Meijer *et al.*[23,24] studied the PCB dynamic flux model of internal lake processes and the process of sediment–water diffusion of PCBs was included in their study. The flux of sediment–water diffusion was larger than that of settling and resuspension for the low molecular weight PCB 28. In contrast, the flux of setting and resuspension was more important than those of sediment–water diffusion for the high molecular weight PCB 153. Therefore, considering only the processes of deposition and resuspension is not sufficient for sediment–water exchange. The process of sediment–water diffusion is very important in controlling water quality.

An understanding of the sediment–water diffusion of PAHs is very important to evaluate the risk of aquatic organism and human expose to environmental contamination. To our knowledge, few studies have investigated the sediment–water diffusion of dissolved PAHs between sediment and water using field experiments. The aim of this study was to quantify the transport trends and to assess equilibrium status of different PAHs at the sediment–water interface in the aquatic environment.

Materials and methods

Chemical and reagents

All solvents used were of pesticide grade purity (J.T. Baker, USA). Silica gel (100–200 mesh) was purchased from Merck (Merck, Germany). Twenty-five PAH standards were purchased from Supelco, Inc. (Supelco, USA), including indene, tetrahydronaphthalene, naphthalene, 2-methylnaphthalene, 1-methylnaphthalene, beta-chloronaphthalene, acenaphthylene, acenaphthene, fluorene, phenanthrene, anthracene, dibenzothiophene, retene, fluoranthene, pyrene, benz(a)anthracene, chrysene, benzo(b)fluoranthene, benzo(k)fluoranthene, benzo(e) pyrene, benzo(a)pyrene, perylene, dibenz(a,h)anthracene, indeno (1,2,3-cd)pyrene, and benzo(g,h,i)perylene. A deuterated PAH solution containing naphthalene-D8, fluorene-D10, pyrene-D10, and perylene-D12 was used as the surrogate standard, and was obtained from Cambridge Isotope Laboratories (CIL, Andover, MA, USA).

Sampling

Dalian, a typical coastal city situated in the northeast of China (E120°58′–123°31′, N38°43′–40°10′), was the urban location selected for this study. A total of 33 surface sediment and sea water samples were collected concurrently from Dalian coastal areas in October, 2008. The locations of the sampling stations are shown in Fig. 1. Subsurface water samples varying from 2–28 m with an average of 6 m from Dalian coastal areas were collected from aboard a chartered vessel. Samples were collected in precleaned 4 L amber glass bottles. Aliquots of each sample were filtered under vacuum after returning to the laboratory to obtain dissolved samples, to which 50 mL of dichloromethane (DCM) were added before PAH extraction to prevent biodegradation and pre-extraction. Surface sediment samples varying from 4–32 m were collected concurrently from the same sites with a grab sampler and stored in prewashed glass bottles. All water and sediment samples were collected in triplicate. The sediment samples were stored at −20 °C until extraction.

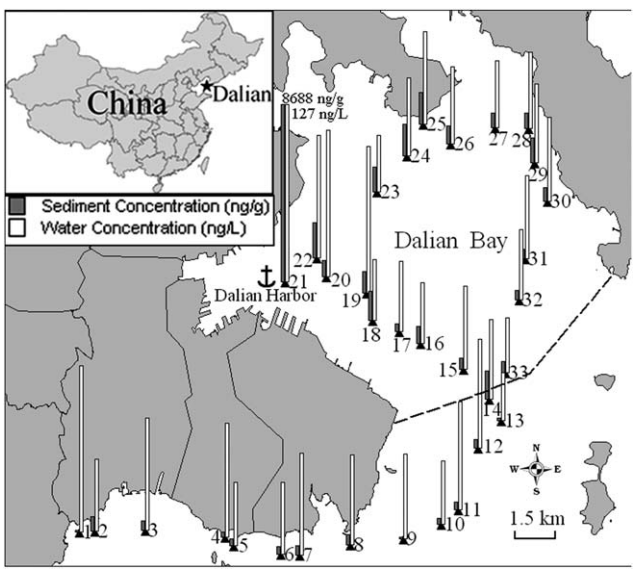

Fig. 1 PAH concentrations in the water and sediment at different sampling sites around Dalian (E120°58′–123°31′, N38°43′–40°10′) coastal areas, China. The dashed line represents the border of Dalian Bay. The highest PAH concentrations in sediment and water were 8688 ng g^{-1} and 127 ng L^{-1} at Site 21 of Dalian Harbor.

Extraction and analyses

Samples were extracted and analyzed according to the methods established at the National Laboratory for Environmental Testing (NLET), Environment Canada.[25,26] Water (4 L) samples spiked with a recovery standard containing a surrogate standard mixture were liquid–liquid extracted using a funnel with 200 mL of DCM. The sediment (10 g) samples spiked with a recovery standard containing a surrogate standard mixture were Soxhlet extracted for 24 h with a 300 mL mixture of n-hexane/acetone (1 : 1, v/v). The extract was filtered through a funnel filled with anhydrous sodium sulfate, and rotary-evaporated to 1 mL. The extract was cleaned-up using a 2-layered packed column (0.4 m length × 10 mm i.d.) filled with anhydrous sodium sulfate (5.0 g, dried for 8 h at 500 °C) and silica gel (10.0 g, dried for 16 h at 135 °C). The column was prewashed with 30 mL of hexane, followed immediately by 30 mL of DCM. The extract was eluted with a 60 mL mixture of hexane/DCM (1 : 1, v/v). The eluate was rotary-evaporated to 2 mL and then reduced into isooctane by nitrogen evaporation (purity 99.999%) prior to gas chromatography-mass spectrometry (GC-MS) analysis. All PAHs were identified and quantified using GC-MS (Thermo, PolarisQ) on a 60-m DB-5 MS column. The column oven temperature was programmed at a rate of 25 °C min^{-1} from an initial temperature of 60 °C to a temperature of 180 °C (1 min hold), and then at 3 °C min^{-1} to 280 °C (30 min hold). The injector, transfer line, and ion source temperatures were 280, 250, and 250 °C, respectively.

Quality assurance/quality control

All samples were spiked with a labeled recovery standard (naphthalene-D8, fluorene-D10, pyrene-D10, and perylene-D12) prior to liquid–liquid extraction and Soxhlet extraction. The surrogate standard recoveries ranged from 58% to 93% and 65% to 96% in liquid–liquid extraction and Soxhlet extraction, respectively. Spike samples were included at a rate of one for every 10 samples extracted, and the recoveries of all 25 PAHs were found to be from 57–102% and 60–110% for liquid–liquid extraction and Soxhlet extraction.

Organic matter fraction in sediment

Ten grams of each sediment sample was isolated for organic matter fraction (φ_{OM}) determination. Firstly, the sediment samples were put into an oven for drying at 105 °C for eight hours until constant weight was achieved. The average moisture of sediment was 45% varying from 26% to 56%. After removing the water, these sediment samples were put into a muffle furnace for φ_{OM} determination by measuring their loss on ignition at 550 °C for five hours. The φ_{OM} of the sediment samples was calculated based on their dry weight and ranged between 2.6% and 10.0% with a mean value of 5.7%.

Results and discussion

PAHs in water and sediment

All PAHs were detected in water and sediment samples except beta-chloronaphthalene. The concentrations of PAHs in water are shown in Table 1 and Fig. 1, ranging from 41 to 127 ng L^{-1} with a mean value of 65 ng L^{-1}. The PAHs in water exhibited a rather uniform distribution of concentrations with a variation of less than one order-of-magnitude. Total concentrations of PAHs in sediment ranged between 113 and 8688 ng g^{-1}, with a mean value of 988 ng g^{-1}. The highest concentration in water was 127 ng L^{-1} at Site 21 of Dalian Harbor. Similarly, the highest concentration in the sediment was also found at Site 21 of Dalian Harbor, which was much higher than those at the other sites.

Generally, the two main factors which influence the concentration distribution of PAHs in sediments are the emission source and the physicochemical properties of the sediments. The organic matter fraction has been implicated as the key physicochemical property influencing PAH content in soil and sediment. A high organic matter fraction usually corresponds with high concentrations of PAHs in sediment or soil.[27,28] Thus, it was necessary to investigate the influence of the organic matter fraction further. The relationship between individual PAH concentration and φ_{OM} of sediment was examined by correlation analysis. The analytical results showed that there was no significant correlation between individual and total concentration of PAHs and φ_{OM} of sediment ($n = 33$). Site 21 had a very high concentration of PAHs and was considered as an outlier on the scatter plot because the correlation increases with this point removed. Significant correlations ($n = 32$, $p<0.05$) were observed between low molecular weight PAHs (indene, naphthalene, 2-methylnaphthalene, 1-methylnaphthalene, and acenaphthylenes) and φ_{OM} of sediment. It was evident that φ_{OM} can affect the distribution of low molecular weight PAHs in sediment. It seems that the emission source along with φ_{OM} played important roles in governing the distribution of PAHs in sediment around Dalian coastal areas. In addition, soot carbon and biogenic sources have influence on the distribution of PAHs in sediment. PAHs are easily accumulated in sediment with high soot carbon content due to their very high affinity for PAHs.[2] Natural sources could also contribute to the elevated PAHs in sediment. These biogenic PAHs such as perylene, phenanthrene, and naphthalene produced by microbial activity in soil could have been transported to water *via* runoff and riverine transport of terrestrial matter.[29]

Variations of PAH concentrations in sediment were observed in different sea areas of Dalian. PAH concentrations at the Dalian Bay sites (Site 15–33) had a mean value of 1379 ng g^{-1}, and were relatively higher in concentration than the other sites (Site 1–14) around the residential and garden areas (mean = 459 ng g^{-1}). The industrial area of Dalian surrounds Dalian Bay, and the industrial wastewater and sewage outlets discharge directly into the sea polluting the water and sediment in Dalian Bay. The higher concentrations of PAHs in Dalian Bay are probably due to this fact. In addition, Dalian Harbor is an important port in Dalian Bay frequently used by naval, commercial and fishing watercrafts, and their emissions may contribute some PAHs to the sediment of Dalian Bay.

As shown in Fig. 2, the composition of PAH congeners were apparently different between water and sediment. In water, 2-methylnaphthalene, 1-methylnaphthalene and naphthalene were the dominant PAHs contributing 40.4% of all PAH concentrations. The top three PAH congeners found in sediment were pyrene, fluoranthene, and phenanthrene, which accounted for 34.4% of the sediment burden. This result was consistent with

Table 1 Concentrations of PAHs in sediment (ng g^{-1}) and water (ng L^{-1}), the logarithm of octanol–water partition coefficients ($\log K_{OW}$), the logarithm of soot carbon–water partition coefficients ($\log K_{SC}$), and fugacity fractions (*ff*) affected by natural organic matter, fugacity fractions ($ff_{1\%SC}$) affected by natural organic matter and soot carbon (1% of organic carbon), and fugacity fractions ($ff_{10\%SC}$) affected by natural organic matter and soot carbon (1% of organic carbon)

			Water			Sediment			*ff*				
PAHs	$\log K_{OW}$[b]	$\log K_{SC}$[c]	Min.	Max.	Mean	Min.	Max.	Mean	Min.	Max.	Mean	$ff_{1\%SC}$ Mean	$ff_{10\%SC}$ Mean
Indene (2)[a]			1.1	3.7	3.7	0.7	20.2	1.4	0.923	0.998	0.980	0.971	0.897
Tetrahydronaphthalene (2)	3.49	5.21	0.8	1.5	1.0	0.3	5.0	1.0	0.739	0.967	0.858	0.800	0.502
Naphthalene (2)	3.37	4.93	2.8	13.4	40.0	1.6	224.1	6.4	0.731	0.998	0.968	0.958	0.880
2-Methylnaphthalene (2)	3.86	5.62	4.4	32.6	19.0	2.1	80.7	12.5	0.303	0.962	0.777	0.699	0.387
1-Methylnaphthalene (2)	3.87	5.63	2.6	17.1	9.2	1.4	47.2	6.9	0.352	0.965	0.770	0.688	0.366
Acenaphthylene (3)	3.94	5.70	0.5	19.5	18.0	1.4	128.2	2.3	0.737	0.993	0.935	0.902	0.701
Acenaphthene (3)	3.92	5.68	0.4	19.6	10.7	0.3	119.4	2.6	0.625	0.994	0.894	0.845	0.583
Fluorene (3)	4.18	5.72	1.5	7.7	20.2	2.0	174.0	3.0	0.504	0.993	0.840	0.800	0.577
Dibenzothiopene (3)	4.29	6.09	1.5	2.3	5.3	1.0	26.6	1.7	0.520	0.960	0.744	0.646	0.306
Phenanthrene (3)	4.57	6.24	1.8	10.6	86.8	10.0	498.5	3.6	0.566	0.991	0.891	0.852	0.631
Anthracene (3)	4.54	6.94	0.9	2.6	34.4	3.1	297.9	1.6	0.667	0.992	0.886	0.700	0.265
Fluoranthene (4)	5.33	6.96	1.0	13.2	109.8	13.0	920.5	2.9	0.628	0.949	0.801	0.740	0.446
Pyrene (4)	5.32	6.79	0.9	12.3	136.0	12.0	1172.0	3.0	0.502	0.946	0.805	0.764	0.528
Retene (3)	6.35	8.33	1.7	2.6	15.4	2.3	186.3	1.9	0.021	0.502	0.056	0.029	0.006
Benzo(a)anthracene (4)	5.91	8.26	0.8	3.4	58.2	3.1	667.6	1.1	0.128	0.916	0.471	0.229	0.042
Chrysene (4)	5.86	8.18	0.6	4.0	66.7	5.0	658.7	1.3	0.271	0.871	0.556	0.299	0.060
Benzo(b)fluoranthene (5)	6.57	8.54	0.6	3.1	55.8	1.5	507.5	1.1	0.022	0.695	0.190	0.111	0.024
Benzo(k)fluoranthene (5)	6.84	8.66	1.2	4.0	58.5	1.6	607.9	1.5	0.007	0.542	0.081	0.051	0.012
Benzo(e)pyrene (5)	6.44	8.28	0.4	3.7	59.8	0.3	656.4	1.0	0.003	0.763	0.163	0.106	0.026
Benzo(a)pyrene (5)	6.30	8.87	0.8	3.7	78.6	2.4	933.7	1.5	0.044	0.868	0.274	0.079	0.011
Perylene (5)	6.25	8.22	N.D.	4.9	15.2	2.3	110.9	0.8	0	0.403	0.077	0.042	0.008
Indeno(1,2,3-cd)pyrene (6)	7.66	9.76	0.6	6.0	38.8	5.0	353.6	1.9	0.002	0.078	0.009	0.004	0.001
Dibenzo(a,h)anthracene (5)	6.75	8.77	0.9	6.5	11.4	1.4	123.4	2.3	0.004	0.200	0.016	0.008	0.001
Benzo(g,h,i)perylene (6)	7.23	8.89	0.8	6.5	36.5	4.4	350	2.0	0.004	0.182	0.022	0.015	0.004

[a] The 2–6 represents the number of PAH ring. [b] The values of $\log K_{OW}$ were calculated using the program of KOWWIN in EPI Suite v3.20 (EPA) or selected from Spero *et al.*,[38] MacKay *et al.*,[39] and Stegmann.[40] [c] The values of $\log K_{SC}$ were calculated using eqn (15) or selected from Bucheli and Gustafsson [44] and Jonker and Koelmans.[45]

a previous study that showed these three compounds accounted for about 32% in the soil of Dalian.[30] The low molecular weight PAH congeners, two- and three-ring PAHs, dominated the profile of PAHs in water. In contrast, the PAH congeners in sediment were mainly medium and high molecular weight PAHs (four- and more than four-ring PAHs).

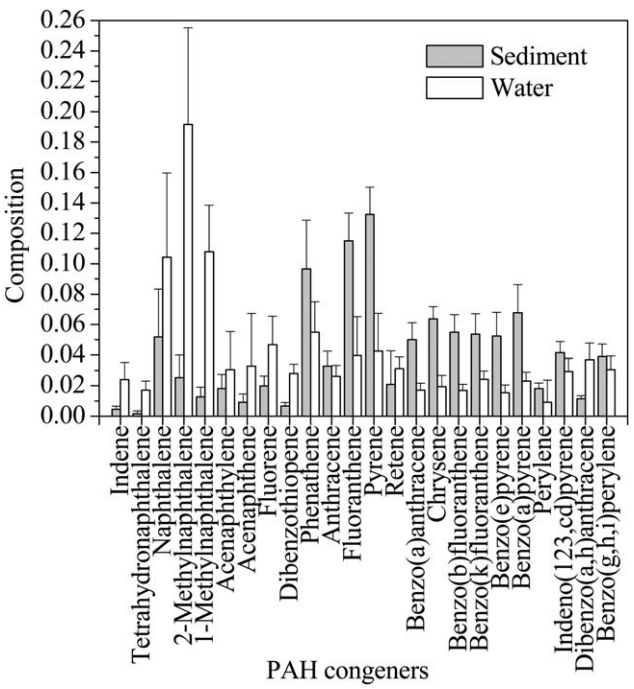

Fig. 2 Composition of PAH congeners in water (ng L^{-1}) and sediment (ng g^{-1}) samples around Dalian coastal areas.

Fugacity fraction calculation

In order to understand the sediment–water diffusion of PAHs, a fugacity approach was used to assess the equilibrium. Fugacity is a measure of chemical potential or partial pressure of a chemical in a particular medium that controls the transfer of chemicals between media.[31] The equilibrium partitioning of a chemical between water and sediment is described by the dimensionless sediment–water partition coefficient (K_{SW}), as follows:

$$K_{SW} = C_S \rho_S / C_W \quad (1)$$

where C_S is the sediment concentration, ρ_S is the density of sediment solids, and C_W is the water concentration.

K_{SW} is dependent on temperature, moisture, chemical, and sediment properties. Partitioning of persistent organic pollutants to sediment occurs *via* absorption to the organic carbon fraction and K_{SW} can be expressed as the product of the organic carbon partition coefficient (K_{OC}) and organic carbon fraction (φ_{OC}), as follows:

$$K_{SW} = K_{OC} \varphi_{OC} \quad (2)$$

K_{OW} is a key parameter of chemical partitioning between the water and organic phase. Many previous studies formulated

a linear relationship that relates K_{OC} to K_{OW} for PAHs and to φ_{OC} of the sediment as follows:[32–34]

$$\log K_{OC} = A \log K_{OW} + B \quad (3)$$

Karickhoff *et al.*[32] obtained values of A of 0.989 and B of −0.346 for PAHs from benzene to pyrene. The values of A of 1.14 and B of −1.02 were derived for PAHs by Nguyen *et al.*[35] Van Noort[36] obtained values of A of 1.11 and B of −1.14 for PAHs. Considering the summarized results, we used the K_{OW} is approximately equal to K_{OC}. According to eqn (3), K_{OW} can be used instead of K_{OC} in eqn (2):

$$K_{SW} = K_{OW}\varphi_{OC} \quad (4)$$

K_{SW} can also be expressed as a ratio of the fugacity capacity (Z-value; mol m^{-3} Pa^{-1}) for sediment (Z_S) and water (Z_W):

$$K_{SW} = Z_S/Z_W \quad (5)$$

The following equation can be used to calculate Z_W values:

$$Z_W = 1/H \quad (6)$$

where H is the Henry law constant. Combining eqn (3)–(6), Z_S can be expressed as:

$$Z_S = K_{OW}\varphi_{OC}/H \quad (7)$$

Fugacities of PAHs in sediment (f_S) and water (f_W) were calculated using eqn (8) and (9) by assuming that the fugacity capacity of sediment is due entirely to the organic matter fraction.[6,9]

$$f_S = C_S\rho_S/Z_S = C_S\rho_S H/\varphi_{OC}K_{OW} \quad (8)$$

$$f_W = C_W/Z_W = C_W H \quad (9)$$

Therefore, the sediment–water fugacity quotient (f_S/f_W) can be calculated as follows (eqn (10)),

$$f_S/f_W = C_S\rho_S/\varphi_{OC}K_{OW}C_W \quad (10)$$

where $f_S/f_W > 1$ indicates net redissolution from sediment into water while $f_S/f_W < 1$ indicates net sorption from water to sediment.

Results are also expressed as the fraction of the total fugacity in sediment (*ff*):

$$ff = f_S/(f_S + f_W) = f_S/f_W/(f_S/f_W + 1) \quad (11)$$

In comparison with the fugacity quotient, a graphical representation of the equilibrium status using the fugacity fraction is advantageous because equivalent deviations from the equilibrium line ($ff = 0.5$) in either direction represent the same magnitude of departure from equilibrium.[6] Sediment–water equilibrium is indicated by a fugacity fraction = 0.5. Values of $ff > 0.5$ indicate net redissolution from sediment into water and values < 0.5 indicate net sorption from water to sediment.

Uncertainty analysis

Model uncertainty is a very important theme for understanding the final fate of a chemical compound using the fugacity model.[6,7] According to eqn (11), the uncertainty of *ff* (u_{ff}) is directly related to the uncertainty of five parameters C_S, ρ_S, φ_{OC}, K_{OW}, and C_W. Notably, three parameters, C_S, K_{OW}, and C_W, have a stronger influence on u_{ff} because their values varied larger than the others. So, u_{ff} is mainly determined by the uncertainty of these three parameters and can be calculated as follows:

$$u_{ff} = \sqrt{\mathrm{RSD}^2(C_S) + \mathrm{RSD}^2(C_W) + \mathrm{RSD}^2(K_{OW})} \quad (12)$$

where RSD is the relative standard deviation. Replicate analyses in our laboratory have shown that the analytical reproducibility in measurements of water and sediment are typically ≈ 35%. de Maagd *et al.*[37] determined the K_{OW} of eight PAHs varying from two-ring naphthalene to five-ring benzo(a)pyrene, and determined that the mean RSD of K_{OW} was 42%. Therefore, assuming 35% RSD in C_W and C_S, and 42% RSD in K_{OW}, the value of u_{ff} was 60% in the *ff* according to eqn (12). The calculation associated with u_{ff} indicated that the equilibrium was represented by the *ff* of 0.5 ± 0.3 (*i.e.*, a range of 0.2–0.8). If the fugacity fractions fall outside this uncertainty range, it can be concluded that these compounds are not in sediment–water equilibrium.

Sediment–water diffusion

Mean PAH concentrations in water and sediment associated with other parameters (Table 1) were used to assess the equilibrium status of each compound. Values of $\log K_{OW}$ were selected in previous studies[38–40] or were calculated using the program of KOWWIN in EPI Suite v3.20 (EPA). The density of dry sediment solids was 1.5 × 10^3 kg m^{-3} for all calculations[41] and φ_{OC} was estimated as 56% of φ_{OM} determined in this study.

Fig. 3A presents the fugacity fractions between sediment and water around Dalian coastal areas, China. The general trend showed that the values of *ff* increased with decreasing molecular weight of PAHs. The values of *ff* for low molecular weight PAHs (two- and three-rings) were > 0.8 except for dibenzothiopene, indicating that the sediment acted as a secondary source to water for these PAHs. The mean value of *ff* for dibenzothiopene was 0.76, which was lower than those of the other three-ring PAHs. Because dibenzothiopene contains one S atom, it was structurally different from the other PAHs in this study. Values of *ff* for four- and five-ring PAHs, for example, benzo(a)anthracene and benzo(a)pyrene, were close to or fell in the range of 0.2–0.8. This implied that medium molecular weight PAHs were close to the sediment–water equilibrium, and that the transfer tendency shifted between sediment and water in different sites. Mean values of *ff* for five- and six-ring PAHs, *e.g.* dibenzo(a,h)anthracene and benzo(g,h,i)perylene, were lower than 0.2, indicating that the sediment acts as a sink for these high molecular weight PAHs from water. The mean value of *ff* for retene was 0.056, which gives it the propensity to partition into sediment. It should be noted that the alkylated PAHs (2-methylnaphthalene, 1-methylnaphthalene, and retene, *i.e.*, 1-methyl-7-isopropyl-phenanthrene) have lower *ff* values than their parent PAHs (naphthalene and phenanthrene), and show

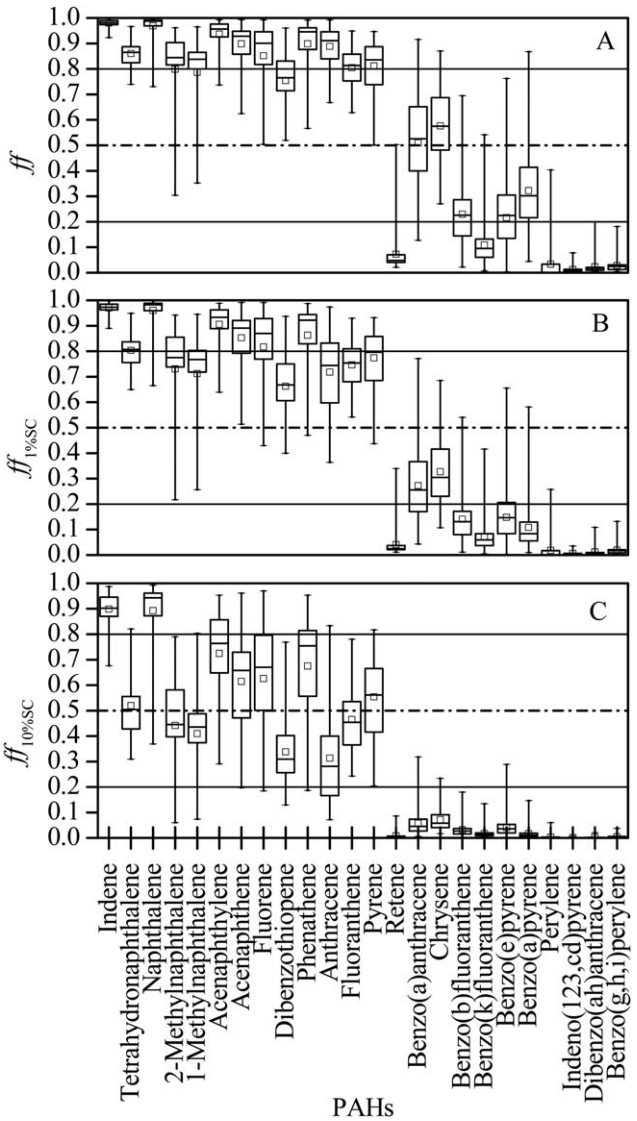

Fig. 3 Fugacity fraction between sediment and water around Dalian coastal areas, China. (A) Fugacity fraction affected by natural organic matter; (B) Fugacity fraction affected by natural organic matter and soot carbon (1% of organic carbon);(C) Fugacity fraction affected by natural organic matter and soot carbon (10% of organic carbon). The bottom and top of the boxes represent the 25th and 75th percentiles of *ff* values, respectively. The solid horizontal line within each box represents the median value. The little box within each box represents the mean value. The lower whisker is equal to the minimum *ff* values. The upper whisker is equal to the maximum *ff* values. The dashed lines of $ff = 0.5$ represent the sediment–water equilibrium status. The dashed lines of $ff = 0.2$ and 0.8 represent uncertainty in the equilibrium condition based on errors propagated in the calculation of *ff*.

a greater tendency to concentrate in sediment rather than water. It is due to the fact that alkylated PAHs have a higher K_{OW} than their parent PAHs (Table 1). The $\log K_{OW}$ are 3.86 for 2-methylnaphthalene, 3.87 for 1-methylnaphthalene, and 6.33 for 1-methyl-7-isopropyl-phenanthrene, which are larger than 3.33 for naphthalene and 4.57 for phenanthrene.

A fugacity fraction in the range of 0.2–0.8 may not represent a significant departure from equilibrium. The uncertainty may be even greater than or perhaps as high as 0.1 to 0.9 if one considers other parameters that are difficult to incorporate into an error analysis, *e.g.*, the uncertainty associated with φ_{OC} and ρ_S in eqn (10). If this characterization of uncertainty is accepted, only indene, naphthalene, acenaphthylene, acenaphthene, phenanthrene, anthracene, retene, perylene, indeno(1,2,3-cd)pyrene, dibenzo(a,h)anthracene, and benzo(g,h,i)perylene would have significant results, which have mean values of *ff* are near or greater than 0.9 or lower than 0.1.

Soot carbon affecting the sediment–water diffusion

In realistic environments, PAHs can be sorbed to not only natural organic matter but also soot carbon.[42] Therefore, soot carbon can affect the sediment–water diffusion of PAHs, which exhibited significantly stronger affinity than natural organic matter.[17] Considering the effect of soot carbon, eqn (2) can be expressed as follows:[42,43]

$$K_{SW} = K_{OC}\varphi_{OC} + K_{SC}\varphi_{SC} \quad (13)$$

where the φ_{SC} is the soot carbon fraction of the sediment and K_{SC} is the soot carbon normalized partition coefficient. Therefore, eqn (10) can be changed as eqn (14) to calculate the fugacity fraction affected by both natural organic matter and soot carbon.

$$f_S/f_W = C_S\rho_S/C_W(K_{OC}\varphi_{OC} + K_{SC}\varphi_{SC}) \quad (14)$$

In the present study, the K_{SC} values reported by Bucheli and Gustafsson[44] and Jonker and Koelmans[45] were used. If K_{SC} for PAHs were not determined by the experiments, the values were calculated using the linear regression of eqn (15) derived from the experimental $\log K_{SC}$ and $\log K_{OW}$ listed in this study. In sediment, φ_{SC} was usually estimated as 1–10% of φ_{OC} determined in previous study.[42]

$$\log K_{SC} = 1.09\log K_{OW} + 1.41 \quad (15)$$

As shown in Fig. 3B and C, the soot carbon have the influence on the transfer trend of PAHs depending on the soot carbon content (soot carbon/organic carbon) varying from 1% to 10%. It seems that soot carbon have a little influence on the transfer trendency of low and high molecular weight PAHs when the sediment with low soot carbon content (1% of φ_{OC}). Most values of $ff_{1\%SC}$ (Table 1) for benzo(a)anthracene, benzo(e)pyrene, and benzo(a)pyrene were lower than 0.2, indicating that transfer tendency of these medium molecular weight PAHs shifted to sediment from the equilibrium. However, the $ff_{10\%SC}$ (Table 1) indicated that the soot carbon changed the tendency of not only the medium molucule weight PAHs but also low molecular weight PAHs. The sediment began to act as a sink for these medium molecular weight PAHs from water and the low molecular weight PAHs reached the sediment-water equilibrium status.

Concentration affecting the sediment-water diffusion

Notably, the difference of PAH concentration between water and sediment can affect their transfer trend. At severely-polluted site

of Dalian Harbor, some PAHs can transfer from sediment to water opposite to other sites at the same equilibrium status (Fig. 4). For example, dibenzothiophene, benzo(a)anthracene, chrysene, and benzo(a)pyrene were net flux from sediment to water which occurs in opposition with their mean sediment-water equilibrium status. Benzo(k)fluoranthene and perylene reached the sediment-water equilibrium status of a net flux from water to sediment at other less polluted sites. We confirmed that a difference in PAH concentrations can change the net flux trend.

Spatial distribution of *ff* for benzo(a)pyrene

Among PAH compounds, benzo[a]pyrene is commonly used as an indicator because its toxicity is one of the highest and it accounts for the majority of the carcinogenicity in a PAH mixture. Therefore,the *ff* of benzo(a)pyrene is a key parameter influencing the risk of marine life living in water. Fig. 5 shows the spatial distribution of *ff* for benzo(a)pyrene around Dalian coastal areas. The value of *ff* varied at different sites. At Site 21 of Dalian Harbor, *ff* was 0.87, which implied a net flux of diffusion of benzo(a)pyrene from sediment to water. Except for Site 21, *ff* for all of the other sites in Dalian Bay were within the range of 0.2–0.8, which meant benzo(a)pyrene reached a dynamic equilibrium status. In contrast to the sites located in Dalian Bay, *ff* for most sites around the residential and garden areas were lower than 0.2, indicating a net flux from water into sediment. These observations suggested that the transfer trend for benzo(a)pyrene was dependent on the PAHs in industrial pollution.

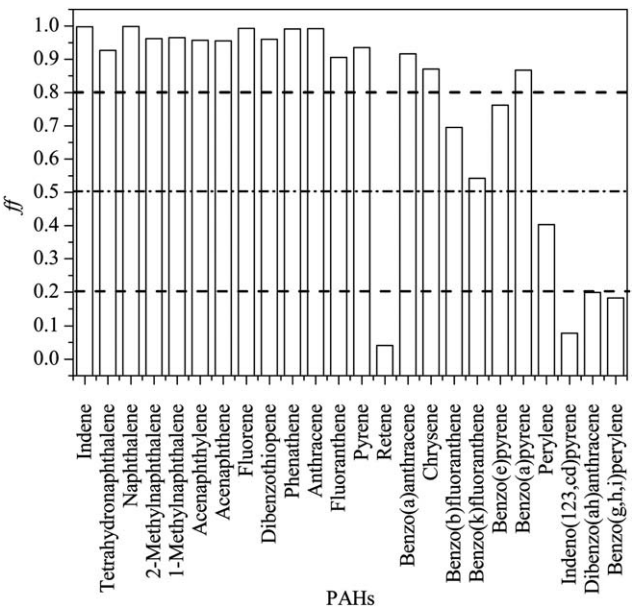

Fig. 4 Fugacity fraction between sediment and water at Site 21 of Dalian Harbor. The dashed lines of $ff = 0.5$ represents the sediment–water equilibrium status. The dashed lines of $ff = 0.2$ and 0.8 represent uncertainty in the equilibrium condition based on errors propagated in the calculation of *ff*.

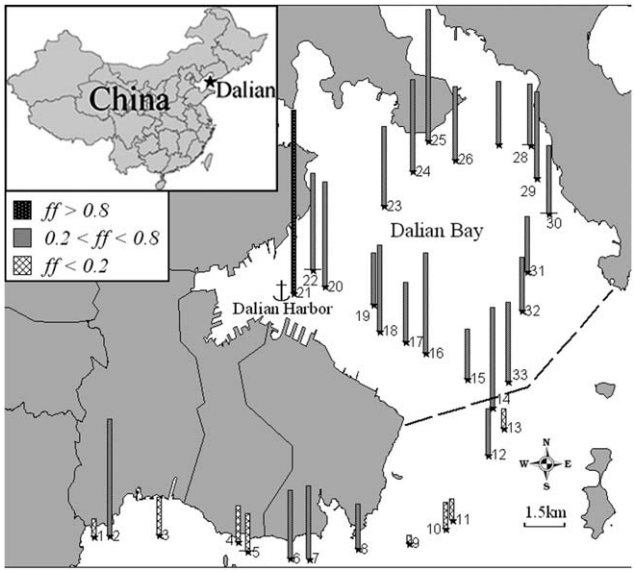

Fig. 5 The spatial distribution of *ff* for benzo(a)pyrene in Dalian coastal areas, China. The dashed line represents the border of Dalian Bay. Values of $ff > 0.8$ indicate net redissolved from sediment and values <0.2 indicate net sorption to sediment. Values in the range of 0.2–0.8 imply that benzo (a)pyrene reaches the equilibrium conditions.

Conclusions

The sediment–water fugacity fractions indicated that sediment acted as a secondary source to the water for all low molecular weight PAHs (two-three rings), and it will continue to be a sink for high molecular weight PAHs (five-six rings) around Dalian coastal areas. Medium molecular weight PAHs (four-five rings) were close to the sediment–water equilibrium and the tendency shifted between sediment and water when the function region changed in Dalian. Soot carbon and the concentrations of PAHs in water and sediment were the main factors affecting the sediment–water equilibrium status. Due to soot carbon content in sediment, the low and medium molecular weight PAHs changed their transfer tendency between sediment and water. In the severely-polluted site, PAHs in sediment had a strong influence on the PAH concentration in water through the process of sediment–water diffusion. According to these results, the process of sediment–water diffusion should be considered in controlling PAH concentration in water. The present fugacity fraction solution to the sediment–water diffusion is best suited for evaluating the diffusion trend of PAHs in aquatic environment.

Acknowledgements

This study was supported by the China National Natural Science Foundation Program (Grant No. 20807008 and 21077015). Dr De-Gao Wang acknowledged the support by the Natural Sciences and Engineering Research Council of Canadian Government Laboratory Visiting Fellowship. The authors thank anonymous reviewers for their comments and suggestions on this work.

References

1 J. Dachs and L. Méjanelle, *Estuaries Coasts*, 2010, **33**, 1–14.
2 J. Dachs and S. J. Eisenreich, *Environ. Sci. Technol.*, 2000, **34**, 3690–3697.

3 E. Jurado, F. Jaward, R. Lohmann, K. C. Jones, R. Simó and J. Dachs, *Environ. Sci. Technol.*, 2005, **39**, 2426–2435.
4 E. Jurado, J. M. Zaldívar, D. Marinov and J. Dachs, *Mar. Pollut. Bull.*, 2007, **54**, 441–451.
5 K. C. Jones, *Environ. Sci. Pollut. Res.*, 1994, **1**, 171–177.
6 T. Harner, T. F. Bidleman, L. M. M. Jantunen and D. Mackay, *Environ. Toxicol. Chem.*, 2001, **20**, 1612–1621.
7 T. Harner, D. Mackay and K. C. Jones, *Environ. Sci. Technol.*, 1995, **29**, 1200–1209.
8 C. Backea, I. T. Cousins and P. Larsson, *Environ. Pollut.*, 2004, **128**, 59–72.
9 T. F. Bidleman and A. D. Leone, *Environ. Pollut.*, 2004, **128**, 49–57.
10 I. T. Cousins and K. C. Jones, *Environ. Pollut.*, 1998, **102**, 105–118.
11 S. N. Meijer, M. Shoeib, L. M. M. Jantunen, K. C. Jones and T. Harner, *Environ. Sci. Technol.*, 2003, **37**, 1292–1299.
12 S. N. Meijer, M. Shoeib, K. C. Jones and T. Harner, *Environ. Sci. Technol.*, 2003, **37**, 1300–1305.
13 W.-H. Cheng, Y.-J. Chou and H.-P. Lin, *J. Environ. Sci. Health., Part A*, 2007, **42**, 129–134.
14 Y.-Z. Tang, W. H. Schroeder, D. Mackay, Q. Tran, M. Chai and H. Van Ooijen, *Int. J. Environ. Anal. Chem.*, 1996, **65**, 169–182.
15 M. Odabasi, B. Cetin, E. Demircioglu and A. Sofuoglu, *Mar. Chem.*, 2008, **109**, 115–129.
16 A. Bozlaker, A. Muezzinoglu and M. Odabasi, *J. Hazard. Mater.*, 2008, **153**, 1093–1102.
17 J. Dachs, S. J. Eisenreich and R. M. Hoff, *Environ. Sci. Technol.*, 2000, **34**, 1095–1102.
18 J. Dachs, S. J. Eisenreich, J. E. Baker, F.-C. Ko and J. D. Jeremiason, *Environ. Sci. Technol.*, 1999, **33**, 3653–3660.
19 D. Mackay, A. Di Guardo, S. Paterson and C. E. Cowan, *Environ. Toxicol. Chem.*, 1996, **15**, 1627–1637.
20 R. Lun, K. Lee, L. De Marco, C. Nalewajko and D. Mackay, *Environ. Toxicol. Chem.*, 1998, **17**, 333–341.
21 J. D. Jeremiason, S. J. Eisenreich, J. E. Baker and B. J. Eadie, *Environ. Sci. Technol.*, 1998, **32**, 3249–3256.
22 A. Palm, I. Cousins, Ö. Gustafsson, J. Axelman, K. Grunder, D. Broman and E. Brorström-Lundén, *Environ. Pollut.*, 2004, **128**, 85–97.
23 S. N. Meijer, J. Dachs, P. Fernandez, L. Camarero, J. Catalan, S. Del Vento, B. van Drooge, E. Jurado and J. O. Grimalt, *Environ. Pollut.*, 2006, **140**, 546–560.
24 S. N. Meijer, J. O. Grimalt, P. Fernandez and J. Dachs, *Environ. Pollut.*, 2009, **157**, 1815–1822.
25 Y. Su, H. Hung, E. Sverko, P. Fellin and H. Li, *Atmos. Environ.*, 2007, **41**, 8725–8735.
26 C. H. Marvin, E. Sverko, M. N. Charlton, P. A. L. Theissen and S. Painter, *J. Great Lakes Res.*, 2004, **30**, 277–286.
27 W. Wilcke, *J. Plant Nutr. Soil Sci.*, 2000, **163**, 229–248.
28 J. J. Nam, G. O. Thomas, F. M. Jaward, E. Steinnes, O. Gustafsson and K. C. Jones, *Chemosphere*, 2008, **70**, 1596–1602.
29 L. Nizzetto, R. Lohmann, R. Gioia, A. Jahnke, C. Temme, J. Dachs, P. Herckes, A. D. Guardo and K. C. Jones, *Environ. Sci. Technol.*, 2008, **42**, 1580–1585.
30 D. Wang, M. Yang, H. Jia, L. Zhou and Y. Li, *J. Environ. Monit.*, 2008, **10**, 1076–1083.
31 S. N. Meijer, T. Harner, P. A. Helm, C. J. Halsall, A. E. Johnston and K. C. Jones, *Environ. Sci. Technol.*, 2001, **35**, 4205–4213.
32 S. W. Karickoff, *Chemosphere*, 1981, **10**, 833–846.
33 A. P. Khodadoust, L. Lei, J. E. Antia, R. Bagchi, M. T. Suidan and H. H. Tabak, *J. Environ. Eng.*, 2005, **131**, 403–409.
34 B. M. Gawlik, N. Sotiriou, E. A. Feicht, S. Schulte-Hostede and A. Kettrup, *Chemosphere*, 1997, **34**, 2525–2551.
35 T. H. Nguyen, K.-U. Goss and W. P. Ball, *Environ. Sci. Technol.*, 2005, **39**, 913–924.
36 P. C. M. van Noort, *Chemosphere*, 2009, **74**, 1018–1023.
37 P. G.-J. de Maagd, D. T. E. M. ten Hulscher, H. van den Heuvel, A. Opperhuizen and D. T. H. M. Sijm, *Environ. Toxicol. Chem.*, 1998, **17**, 251–257.
38 J. Spero, B. Devito and L. Theodore, *Regulatory chemicals handbook*, CRC Press, New York, 2000.
39 D. Mackay, W. Shiu and K. Ma, *Illustrated Handbook of Physical-Chemical Properties and Environmental Fate for Organic Chemicals*, Lewis, London, 1998.
40 R. Stegmann, *Treatment of contaminated soil: fundamentals, analysis, applications*, Springer, Berlin Heidelberg, 2001.
41 D. Mackay, *Multimedia environmental models: The fugacity approach*, 2nd edn, CRC Press, Boca Raton, Florida 2001.
42 Ö. Gustafsson, F. Haghseta, C. Chan, J. MacFarlane and P. M. Gschwend, *Environ. Sci. Technol.*, 1997, **31**, 203–209.
43 S. Ribes, B. Van Drooge, J. Dachs, O. Gustafsson and J. O. Grimalt, *Environ. Sci. Technol.*, 2003, **37**, 2675–2680.
44 T. D. Bucheli and Ö. Gustafsson, *Environ. Sci. Technol.*, 2000, **34**, 5144–5151.
45 M. T. O. Jonker and A. A. Koelmans, *Environ. Sci. Technol.*, 2001, **35**, 3742–3748.

